Volume 22, No 3 | International Journal of Radiation Research, July 2024

The Application of 3.0 T magnetic resonance perfusion-weighted imaging in the differentiation and grading of brain gliomas

L. Zhang and M. Sun*

Department of Magnetic Resonance Imaging, Cangzhou Central Hospital, No. 16 Xinhua West Road, Cangzhou City 061001, Hebei Province, China

► ***Original article***

Corresponding author:
Dr. M. Sun
E-mail: *Smin_1201@163.com*

Received: August 2023
Final revised: December 2023
Accepted: January 2024

Int. J. Radiat. Res., July 2024; 22(3): 573-578

DOI: 10.61186/ijrr.22.3.573

Keywords: *Perfusion Weighted MRI, glioma, neoplasm grading, diagnosis.*

ABSTRACT

Background: To investigate the value of 3.0T magnetic resonance perfusion-weighted imaging (PWI) in the preoperative differential diagnosis and grading assessment of gliomas. ***Materials and Methods:*** The PWI features of 23 single brain metastases and 73 gliomas (32 low-grade and 41 high-grade) were retrospectively analyzed with postoperative pathological findings. The cerebral blood volume (CBV) values of the tumour parenchyma, the peritumoral oedema area and the contralateral normal brain tissue were measured, and the relative CBV (rCBV) values were calculated and statistically analysed. ***Results:*** A total of 96 patients, comprising 66 men and 30 women with a mean age of 47 ± 11 years, were included in the study. The time-signal curves of gliomas of different grades obtained by magnetic resonance perfusion have different characteristics. The rCBV values for tumor parenchyma and peritumoral edema were higher in the high-grade glioma group than in the low-grade glioma group and the single brain metastasis group ([6.01 ± 1.64] vs [2.16 ± 0.87] vs [4.37 ± 1.03]) and ([1.82 ± 0.47] vs [0.79 ± 0.34] vs [0.81 ± 0.21]), and the differences were significant ($p < 0.05$). The rCBV value of the tumour parenchyma in the single brain metastasis group was higher than that in the low-grade glioma group ([4.37 ± 1.03] vs [2.16 ± 0.87]), and the difference was significant ($p < 0.05$). ***Conclusion:*** Magnetic resonance PWI has high clinical value in the preoperative diagnosis and grading evaluation of gliomas.

INTRODUCTION

A glioma is a common intracranial malignant tumour, accounting for approximately 40% of all intracranial tumours, showing infiltrative growth and unclear boundaries with normal brain tissue. According to the World Health Organization (WHO) classification [1], gliomas can be divided into WHO grade I–IV; grades I and II are considered as low-grade gliomas, and grades III and IV are considered as high-grade gliomas. There are significant differences in the prognosis of the different grades. For example, WHO grade I has low proliferation ability and may be cured by surgery. However, WHO grade II is an invasive tumour, and, although the proliferative activity is low, relapse can easily occur, and there is a tendency to develop into a higher-grade malignant tumour. Surgery, followed by postoperative adjuvant radiotherapy, is generally the main clinical treatment [2]. The treatment plan and surgical methods for intracranial tumours at different sites, different grades and of different natures are not the same, and there are significant differences in prognosis. Determining how to safely remove the tumour to the greatest extent has always been difficult [3]. Therefore, timely and accurate preoperative diagnosis of gliomas and evaluation of their grade are crucial for the selection of treatment options and the prognosis of patients.

The clinical and imaging findings of gliomas suffer from a lack of specificity, especially with grade II–IV gliomas, which can be characterised by unclear boundaries and varying degrees of mixed-signal imaging with necrosis and cystic degeneration. In addition, single brain metastases without a clear primary history and typical imaging findings are difficult to distinguish from high-grade gliomas. Conventional magnetic resonance scans can show the location and approximate extent of the tumor, but the grading of glioma cannot make a diagnosis [4]. pathological diagnostic methods are invasive and needle biopsy results depend on the material site and sample size, which is difficult to reflect the entire tumor [5]. Functional magnetic resonance imaging compensates for the lack of conventional magnetic resonance imaging and pathological tissue diagnosis. In recent years, with the development of medical imaging technology, many researchers have distinguished perfusion-weighted imaging (PWI) from magnetic resonance spectroscopy (MRS) with some clinical relevance [6]. However, MRS has high technical requirements for the operator, a long

[DOI: 10.61186/ijrr.22.3.573]

examination time and often unstable spectral line results. Perfusion-weighted imaging has been widely used in the diagnosis of central nervous system diseases due to its high stability, reliable results, short examination time and ready acceptance by patients [7]. As a new noninvasive technique to measure cerebral perfusion, PWI can be used to reflect the hemodynamic changes of brain tissue. The malignant degree of glioma is closely related to the number of blood vessels in the tumor, and the degree of vascular proliferation in high-grade glioma is significantly higher than that in low-grade glioma, so PWI can provide more diagnostic information of glioma grade than conventional MRI [8,9]. Therefore, the novelty of this study lies in the use of PWI for the diagnostic grading of glioma, compared with previous studies using conventional MRI, using a new method, can make up for the lack of conventional magnetic resonance and pathological tissue diagnosis.

This study addresses the limitations of current diagnostic methods by using advanced magnetic resonance PWI. This technology's stability, speed and patient-friendliness offer a promising solution to the challenges of distinguishing gliomas from brain metastases, potentially revolutionising clinical practice and improving patient outcomes.

MATERIALS AND METHODS

Study participants

A convenience sampling method was used to select 96 patients with gliomas or single brain metastases from the hospital between January 1, 2018 and October 31, 2022 for the study. All eligible patients underwent conventional magnetic resonance imaging (MRI) plain scans, enhancement and PWI scans for preoperative grading evaluation. Postoperative pathological examinations, including pathological section and immunohistochemistry, were performed to determine their pathological type and WHO pathological grade. Inclusion criteria: 1) confirmation of glioma or solitary brain metastasis through surgery and pathology; 2) absence of MRI contraindications and no prior tumour intervention or treatment before MRI; and 3) surgery or biopsy performed within 2 weeks after MRI examination with obtainment of pathological results. The exclusion criteria included the following 1) unknown clinicopathological results and 2) presence of image artifacts preventing analysis. Ethical approval was obtained from the Medical Ethics Committee of Cangzhou Central Hospital (Ethical number: 2021-020-02 [z]; review and approval date: 16 March 2021).

Instruments and methods

All patients underwent MRI scans of the brain on a 3.0T magnetic resonance scanner (GE Discovery MR750, GE Company, USA) equipped with a 16-channel phased array coil. Patients were placed in the supine position with head tilted forward, and an anterior combined posterior line was used as a positioning line to ensure that the axial scanning direction was the same for all sequences.

MRI scans were performed using a T1-weighted image fluid-attenuated inversion recovery (T1WI FLAIR) sequence with parameters set at repetition time (TR) =2,000 ms, echo time (TE) =24 ms, field of view (FOV) = 220×220 mm, slice thickness =6 mm, and interslice distance =1 mm; T2WI sequence parameters were TR = 6,400 ms, TE = 94 ms, FOV =220×220 mm, slice thickness = 6 mm, and interslice distance =1 mm; T2FLAIR sequence parameters were set at TR = 9,000 ms, TE =90 ms, inversion time (TI =2,500 ms), FOV =220×220 mm, slice thickness =6 mm, and interslice distance = 1 mm.

PWI scans were performed using a gradient echo scan sequence with scan parameters TR =1500 ms, TE = 30 ms, FOV = 220×220 mm, slice thickness = 5 mm, and slice spacing =1 mm. Each patient was scanned with 20 layers, and each layer was scanned for 60 phases. When scanning to the second phase, the contrast agent gadobenate dimeglumine (Gd-BOPTA) (Qiyue Biological Co., Ltd., Xi'an) was injected at a dose of 0.1 – 0.2 mmol/kg, with an injection rate of 3–4 mL/s and an injection time of < 5 s, and 20 mL of normal saline was injected at the same rate.

Images post-processing method

Following PWI scanning, the data were transferred to a GE workstation (Spectris Solaris EP, Shanghai Sanwei Medical Equipment Co., Ltd., USA) for post-processing, and a CBV false colour map was reconstructed for selected levels. In the CBV false colour map, red represented the perfusion area with the highest blood flow, followed by yellow, green and blue, while/black indicated perfusion-deficient or non-perfusion areas. A T1WI flair-enhanced image was used as a reference to avoid large blood vessels, bleeding, calcification, cystic and other areas, and the maximum perfusion level was selected. Three regions of interest (ROI) of 30–40 mm^2 were selected from the maximum perfusion area of the tumour parenchyma, the oedema area around the tumour and the contralateral normal white matter area by two doctors with 10 years and 5 years of neuroimaging experience, respectively [3,6]. The ROIs were selected in the area with the highest CBV value on the CBV map, and the CBV value was calculated. The maximum value (CBVmax) of the lesion and the surrounding oedema area was taken in the solid area of the lesion and the oedema area around the tumour. The rCBV values of the tumour parenchymal area and the peritumoral oedema area were calculated based on the CBV values of the contralateral normal brain tissue. The rCBV value was calculated as (CBV value

[DOI: 10.61186/ijrr.22.3.573]

of tumour parenchyma or peritumoral oedema area/ CBV value of contralateral normal white matter).

Pathological examination

Intraoperative tumor specimens were fixed in 10% formaldehyde solution (5 um thick paraffin sections) and washed with PBS. Sections were heated and boiled in 10 ml sodium citrate buffer (pH 6.0) for 1 min, then immersed in warm water below the boiling point for 9 min and washed with PBS. Sections were incubated in 1% hydrogen peroxide solution for 10 min, endogenous peroxidase was removed and washed with PBS. Blocking was performed with blocking solution at room temperature for 1 h. After removing the blocking solution by aspiration, the sections were incubated in an incubator for 30 min and washed with PBS. After routine staining of the sections with hematoxylin and eosin, gradient alcohol dehydration, and deparaffinization with xylene solution, slides were mounted with coverslips and observed under a microscope (Olympus, Japan, type IX71) (all immunohistochemical reagents were provided by Fujian Maixin Biotechnology Co., Ltd.). Pathologic classification of all tumor specimens was performed by two experienced senior neuropathologists. A WHO qualitative classification was performed according to the 2021 WHO classification criteria (WHO CNS5) for central nervous system tumours [10]. If the opinions of the two physicians were inconsistent, the section consultation was determined by the pathology department.

Statistical methods

SPSS 20.0 software was used for statistical analysis. All data showed as mean ± SD. One-way analysis of variance was performed on low-grade glioma, high-grade glioma and single brain metastasis data, and the least significant difference method was used for pairwise comparison in post-hoc analysis. $p < 0.05$ was considered statistically significant.

RESULTS

Basic information and characteristics

There were 96 patients, 66 males and 30 females. Mean age was 47 ± 11 years. Clinical symptoms include vomiting, headache, epilepsy, movement and sensory disorders.

The results were 32 cases of low-grade glioma (grade I–II), including astrocytoma (25 cases), oligodendroglioma(6 cases) and ependymoma(one case). There were 41 cases of high-grade glioma (grade III–IV), including astrocytoma (29 cases), oligodendroglioma (11 cases) and ependymal (one case). There were 23 cases of single brain metastasis (table 1). (Immunohistochemistry results in some patients are shown in figure 1A-E).

Table 1. Demographic information of patients.

N/`X±S	
Gender (male / female)	66/30
Age	47±11
Pathological grade of the gliomas	
Low grade glioma (grade I-II)	32
astrocytoma	25
oligodendroglioma	6
ependymocytoma	1
High grade glioma (grade I-II)	41
astrocytoma	29
oligodendroglioma	11
ependymocytoma	1
Single brain metastases	23

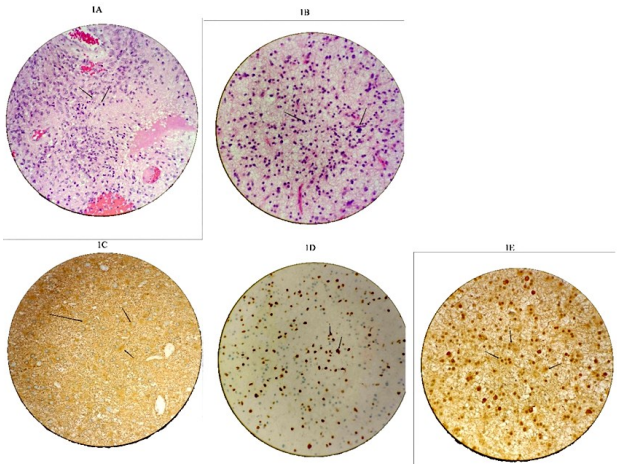

Figure 1. Immunohistochemical images (the magnification was 100x). **A:** grade III glioma; **B:** grade II glioma; **C:** immunohistochemical GFAP (+) for astrocytoma; **D:** immunohistochemical Olig-2(+) for astrocytoma; **E:** immunohistochemical S-100 (+) for astrocytoma.

Magnetic resonance imaging features of gliomas at different grades

The low-grade colloids in the tumour parenchyma had negative enhancement, mainly due to low signal. The descending branch and ascending branch of the curve in the lesion area were asymmetric, rose rapidly and returned to the baseline level. Some areas showed hyperperfusion and cystic areas showed hypoperfusion (figures 2A - C).

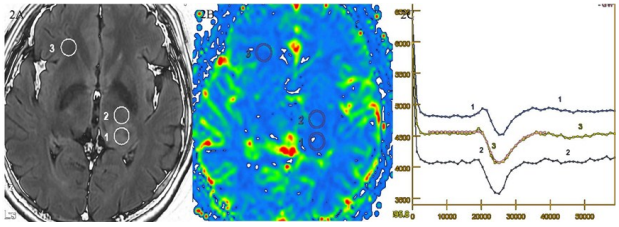

Figure 2. Magnetic resonance perfusion pseudocolor map and time-signal curve (tumor parenchyma). **A**, **B** and **C** are the rCBF, rCBV maps and kinetic curves obtained after PWI post-processing, respectively.

High-grade gliomas exhibited significant negative enhancement in the parenchymal area of the tumour, with predominantly high signal intensity. The curve of the lesion area decreased significantly, increased

[DOI: 10.61186/ijrr.22.3.573]

slowly and could not return to the baseline level; perfusion was heterogeneous, and the liquefied necrotic area of the tumour showed perfusion loss (figures 3A - C).

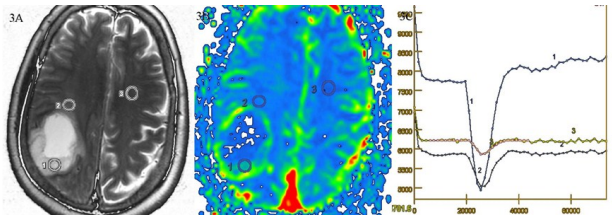

Figure 3. Magnetic resonance perfusion pseudocolor map and time-signal curve (high-grade gliomas). **A**, **B** and **C** are the rCBF, rCBV maps and kinetic curves obtained after PWI post-processing, respectively.

Single brain metastases exhibited negative enhancement in the parenchymal area of the tumour. The time to return to the baseline level of the curve was longer than normal, perfusion was heterogeneous and the liquefied necrotic area of the tumour showed hypoperfusion or isoperfusion (figures 4A - C).

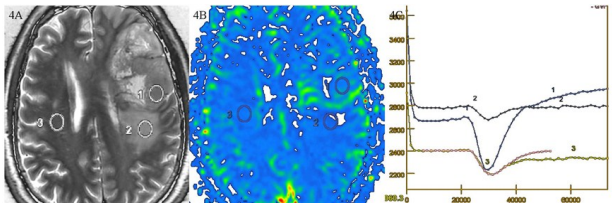

Figure 4. Magnetic resonance perfusion pseudocolor map and time-signal curve (single brain metastases). **A**, **B** and **C** are the rCBF, rCBV maps and kinetic curves obtained after PWI post-processing, respectively.

Comparison of relative cerebral blood volume values between gliomas at all levels and single brain metastases

Different rCBV values in the parenchymal and peritumoral edema areas of the tumor in the glioma group and the single brain metastasis group at each grade level ($F = 16.685$, $p < 0.001$; $F = 6.358$, $p = 0.003$). On pairwise comparison, the rCBV values in the high-grade glioma group were higher than those in the low-grade glioma group and the single brain metastasis group ([6.01 ± 1.64] vs [2.16 ± 0.87] vs [4.37 ± 1.03]) and ([1.82 ± 0.47] vs [0.79 ± 0.34] vs [0.81 ± 0.21]) in both the parenchymal and peritumoral oedema areas ($p < 0.05$). The rCBV values in the tumour parenchymal area were higher in the single brain metastasis group than in the low-grade glioma group ([4.37 ± 1.03] vs [2.16 ± 0.87]), and the differences were significant ($p < 0.05$). There was no obvious difference in rCBV values between the peritumoral oedema area between the single brain metastasis group and the low-grade glioma group ($p > 0.05$) (table 2).

Table 2. Comparison of rCBV values between gliomas at all levels and single brain metastases.

low-grade glioma group	high-grade glioma group	single brain metastasis group	F	P	
parenchymal	2.16±0.87a	6.01±1.64b	4.37±1.03ba	16.685	0.001
peritumoral edema areas	0.79±0.34a	1.82±0.47b	0.81±0.21a	6.358	0.003

DISCUSSION

Gliomas are one of the most abundant tumours in vivo. The growth and infiltration of tumour cells are closely related to tumour vascularity and neovascularisation. Brem *et al.* [11] first proposed a positive correlation between tumor grade and the degree of tumor angiogenesis, with the higher the degree of vascular proliferation, the higher the glioma grade. Vascular endothelial growth factor (VEGF) in gliomas is closely related to microvessel density (MVD). Previous studies have confirmed that the degree of vascular proliferation in gliomas is associated with their malignancy and is one of the important parameters determining the pathological grade [12–14]. At present, VEGF and MVD are mostly used to evaluate the angiogenesis of gliomas in clinical work, but this method can only be used after surgery during laboratory determination of resected tumour specimens.

The results showed that the rCBV values in the parenchymal and peritumoral edema areas of tumors in the low-grade glioma group were significantly lower than those in the high-grade glioma group. The reason for this may be that the growth pattern of the glioma was infiltrative growth or central expansive, surrounding infiltrative growth [15], and there was no clear demarcation between the tumour parenchyma and the surrounding normal brain tissue. The significant increase in the rCBV value in the parenchymal area of high-grade glioma tumours indicates that the higher the malignancy of gliomas, the richer its tumour cell blood supply. The increased blood volume in the peritumoral oedema area of high-grade gliomas is closely related to the infiltration of tumour vessels [16], and the infiltration of tumour vessels is the main cause of increased blood perfusion in the peritumoral oedema area [17]. There are also differences in rCBV values in peritumoral oedema areas, and it is possible that the formation mechanism of peritumoral oedema areas in gliomas is not only local formation of vasogenic oedema caused by irregular and disrupted blood-brain barrier of new tumour vessels (high rCBV values) [18] but also cytotoxic oedema caused by abnormal metabolism of cells in distant tumour areas due to biological factors secreted by tumours (low rCBV values). Therefore, the rCBV values of peritumoral oedema in gliomas of

[DOI: 10.61186/ijrr.22.3.573]

different grades vary according to the degree of infiltration. According to this, the measurement of rCBV in the peritumoral oedema area by PWI can be used as an effective new method to differentiate different grades of gliomas. It has also been shown that there is a good correlation between rCBV measured by PWI and the pathological parameters MVD and VEGF [19]. Perfusion-weighted imaging involves performing a rapid MRI scan after an intravenous bolus injection of a paramagnetic contrast agent to obtain images of the first-pass ROI of the contrast agent. Compared with the limitations of conventional MRI and enhanced scans whereby they do not truly reflect the degree of tumour vascular proliferation and vascular permeability [20], PWI is more advantageous in this regard.

This study also found that the rCBV value of high-grade gliomas was higher in the parenchymal area of the tumour than in single brain metastases, indicating that the glioma blood supply was richer than metastases, which was consistent with the pathological findings of gliomas [21]. In the peritumoral oedema area, this study suggested that the rCBV value of high-grade gliomas was higher than that of single brain metastases, and the difference was significant, which was consistent with the relevant literature reports [22]. Most of the oedema areas around high-grade gliomas showed hyperperfusion and were more extensive than conventional and enhanced scans because gliomas had the characteristics of infiltration and growth, and the appearance of oedema areas around tumours was caused by tumour angiogenesis and increased vascular permeability. Therefore, the higher the grade of glioma, the more obvious the invasive generation and the higher the perfusion of the oedema area around the tumour. However, the metastases showed expansive growth, the tumour cells did not infiltrate around, and the oedema area around the tumour was due to vasogenic oedema formation and also compressed the surrounding vessels, causing decreased blood flow. This resulted in hypoperfusion in the oedema area around the metastases, and its rCBV value was lower than that of the contralateral normal brain tissue. The value of rCBV in the peritumoral oedema area in the differential diagnosis of high-grade gliomas and single brain metastases was greater than that in the tumour parenchymal area.

Many methods are used to reflect cerebral blood perfusion imaging, mainly including xenon-enhanced computed tomography (Xe-CT), positron emission tomography (PET), single-photon emission computed tomography (SPECT), CT perfusion and MR perfusion. An Xe-CT scan is a CT scan that uses inert gas Xe to easily cross the blood-brain barrier as a diffusion tracer and can assess regional brain tissue blood flow. However, its operation is complex, it has potential anaesthetic effects, the results are easily affected by respiratory rate and only one parameter of cerebral blood flow can be obtained; therefore, it has been rarely used in clinical practice. Both PET and SPECT belong to radionuclide imaging. The former is considered to be the 'gold standard' of brain tissue function and brain metabolism and functional imaging; molecular imaging and gene imaging can also be performed in the field of molecular biology. However, PET equipment is large, expensive and difficult to use as part of a routine preoperative examination. Furthermore, the procedures involved in SPECT are complex, have low spatial resolution and have long examination times [23]. At present, the most commonly used perfusion imaging methods for imaging are CT perfusion imaging (CTPI) and magnetic resonance PWI, which are used to evaluate the degree of neovascularisation of brain tumours, the nature of tumour lesions and pathological grades and monitor tumour treatment. Previous CTPI is also of high clinical value in the characterisation and grading of tumours [24]. However, compared with CTPI, PWI has no radiation and iodine contrast adverse reactions, especially for paediatric gliomas, and can be used as a noninvasive examination and evaluation method. In addition, MRI has a wide anatomical coverage, which allows for comprehensively reflecting the heterogeneity of the tumour. Some studies have shown that the diagnostic effect of PWI, especially in the peritumoral oedema area is slightly better than that of CTPI, which may be because MRI has a higher resolution for soft tissue and is more intuitive and clearer for the display of peritumoral oedema than CT. In addition, high-grade gliomas infiltrate the surrounding areas heterogeneously and may appear to be isodense on CT images and are difficult to distinguish, meaning ROIs selected for CTPI may measure true oedema areas rather than tumour infiltration areas, leading to underestimation of rCBV values in oedema areas around tumours and reducing their differential diagnostic value [25].

This study has some limitations. First, the PWI features of single brain metastases of different pathological types were not investigated separately, while no further grading comparative study was performed for grade I, II, III and IV gliomas, which may cause a shift in parameter settings. Furthermore, no statistical analysis was performed according to age and gender. Observed participants will be added in subsequent research, and magnetic resonance perfusion parameters of gliomas of different grades, pathological types and sites will be compared and analysed.

CONCLUSION

The rCBV values obtained by magnetic resonance PWI in the tumour parenchymal area and

[DOI: 10.61186/ijrr.22.3.573]

peritumoral oedema area have guiding significance in the preoperative grading evaluation of gliomas. The rCBV values obtained by PWI in the parenchymal and peritumoral oedema areas of the tumour have differential diagnostic values for high-grade gliomas and single brain metastases. The time-signal curves obtained by magnetic resonance PWI have different characteristics in gliomas.

ACKNOWLEDGMENTS

None.

Ethics approval and consent to participate: The study was approved by the Ethics Committee of Cangzhou Central Hospital, batch number: 2021-020-02 (z). Informed consent was obtained from all participants. Reviewed and approved 16 March 2021.

Funding: Not applicable.

Availability of data and materials: Data not directly reported in this publication can be obtained from the corresponding author upon reasonable request.

Conflicts of interest: The authors report no conflicts of interest related to this study.

Authors' contributions: Sun M conceived of the study, and Zhang L participated in its design and coordination, and Sun M & Zhang L drew the manuscript. All authors read and approved the final manuscript.

REFERENCES

1. Chinese Society of Radiation Oncology Therapy (2017) Chinese expert consensus on radiotherapy for glioma. *Chinese Journal of Radiation Oncology* ***27(2):****123-131.*
2. Bahar RC, Merkaj S, Cassinelli Petersen GI, *et al.* (2022) Machine learning models for classifying high-and low-grade gliomas: A systematic review and quality of reporting analysis. *Front Oncol,* ***12:*** *856231.*
3. Chanbour H, Chotai S. Review of Intraoperative Adjuncts for Maximal Safe Resection of Gliomas and Its Impact on Outcomes. *Cancers(Basel).2022;****14(22):****5705.*
4. Soliman RK, Gamal SA, Essa AA, *et al.* Preoperative grading of glioma using dynamic susceptibility contrast MRI: Relative cerebral blood volume analysis of intra-tumoural and peri-tumoural tissue [J]. *Clin Neurol Neurosurg, 2018,* ***167:*** *86-92.*
5. Chai M and Ma D. Application value of functional magnetic resonance imaging in the diagnosis of glioma [J]. *Shaanxi Medical Journal, 2019,* ***48:****603-606.*
6. Ziming Y, Jianjun S, Qiuyan X, *et al.* (2018) Diagnostic value of DWI combined with MRS in viral encephalitis and low grade glioma. *Hinese Journal of CT and MRI* ***16(1):****15-18.*
7. Xinyao H, Xifeng Y, Yan S, *et al.* (2021) Value of diffusion-weighted imaging and perfusion-weighted imaging in differential diagnosis between atypical encephalitis and low-grade glioma. *Lingnan Modern Clinics in Surgery* ***21(4):****437-444.*
8. Kerkhof M, Hagenbeek RE, van der Kallen BFW, *et al.* Interobserver variability in the radiological assessment of magnetic resonance imaging (MRI) including perfusion MRI in glioblastoma multiforme [J]. *Eur J Neurol, 2016,* ***23:*** *1528-1533.*
9. Verger A, Filss CP, Lohmann P, *et al*. Comparison of 18F-FET PET and perfusion-weighted MRI for glioma grading: A hybrid PET/MR study[J]. *Eur J Nucl Med Mol Imaging, 2017,* ***44:*** *2257-2265.*
10. Figarella-Branger D, Appay R, Metais A, *et al.* La classification de l'OMS 2021 des tumeurs du système nerveux central [The 2021 WHO classification of tumours of the central nervous system]. *Ann Pathol. 2022;****42(5):****367-382. doi: 10.1016/ j.annpat.2021.11.005*
11. Brem S, Cotran R, Folkman J (1972) Tumor angiogenesis: a quantitative method for histologic grading. *Journal of the National Cancer Institute,* ***48(2):****347-356.*
12. Seyedmirzaei H, Shobeiri P, Turgut M, *et al.* (2020) VEGF levels in patients with glioma: a systematic review and meta-analysis. *Reviews in the neurosciences,* ***32(2):****191-202.*
13. Ishikawa E, Miyazaki T (2021) Benefits and Prospects of VEGF-targeted Anti-angiogenic Therapy and Immunotherapy for High-grade Glioma. *No Shinkei Geka* ***49(3):****597-607.*
14. Li M, Liu Y, Dong L, *et al*. (2021) MRI texture analysis in predicting MGMT protein expression in glioblastoma patients. *Journal of Practical Radiology* ***37(1):****9-12.*
15. Park JE, Ryu KH, Kim HS, *et al.* (2017) Perfusion of surgical cavity wall enhancement in early post-treatment MR imaging may stratify the time-to-progression in glioblastoma. *PLoS One* ***12(7):*** *e0181933.*
16. Watkins S, Robel S, Kimbrough IF, *et al*. (2014) Disruption of astrocyte-vascular coupling and the blood-brain barrier by invading glioma cells. *Nature communications* ***5:****4196.*
17. Server A, Orheim TE, Graff BA, *et al*. (2011) Diagnostic examination performance by using microvascular leakage, cerebral blood volume, and blood flow derived from 3-T dynamic susceptibility-weighted contrast-enhanced perfusion MR imaging in the differentiation of glioblastoma multiforme and brain metastasis. *Neuroradiology,* ***53(5):****319-330.*
18. Grist JT, Withey S, MacPherson L, *et al*. (2020) Distinguishing between paediatric brain tumour types using multi-parametric magnetic resonance imaging and machine learning: A multi-site study. *NeuroImage Clinical,* ***25:****102172.*
19. Haris M, Husain N, Singh A, *et al*. (2008) Dynamic contrast-enhanced derived cerebral blood volume correlates better with leak correction than with no correction for vascular endothelial growth factor, microvascular density, and grading of astrocytoma. *Journal of computer assisted tomography,* ***32(6):****955-965.*
20. Huo Chengcun (2021) Diagnostic Value and Imaging Characteristics of Perfusion Weighted Imaging in Central Nervous System. *Imaging research and medical applications,* ***5(12):****148-149.*
21. Wesseling P, Ruiter DJ, Burger PC (1997) Angiogenesis in brain tumors; pathobiological and clinical aspects. *Journal of neuro-oncology,* ***32(3):****253-265.*
22. Jieyun C, Xiaoying L, Xiangrong C, *et al*. (2015) Differential diagnosis of solitary brain metastases and high-grade gliomas by MR perfusion weighted imaging. *Chinese Journal of Medical Imaging Technology,* ***31(2):****215-218.*
23. Yang L (2015) Progress of Brain CT Perfusion Imaging. *Chinese Journal of Medical Imaging Technology,* ***31(5):****779-782.*
24. Liang X, Du C, Bin J, *et al*. (2015) Value of 128-slice spiral CT perfusion imaging in glioma grading and postoperative follow-up. *Chinese Journal of Neurosurgery,* ***31(5):****505-507.*
25. Kang L, Zhang Y, Sun S (2007) Preliminary comparative study of CT perfusion imaging and MR perfusion imaging in peritumoral edema. *Journal of Clinical Radiology,* ***26(4):****319-322.*

[DOI: 10.61186/ijrr.22.3.573]